Two-Tier Steady-State Cosmology and the Discovery of a Universal Scaling Law: QIC-S Theory Ver 9.1

Yoshiaki Sasada

February 4, 2026

Abstract

We present a unified theoretical framework, Quantum Information Cosmology (QIC-S), that accounts for galactic rotation curves without invoking particle dark matter. This theory reconceptualizes the universe as a **Two-Tier System**: Tier 1 (Regenerative Cosmology) governs cyclic galactic evolution through six distinct phases, while Tier 2 (New Steady-State Cosmology) maintains global cosmic stationarity via the Cosmic Web.

In this work, we establish two definitive observational validations:

(1) Statistical Verification at Galactic Scales ($N = 170$): Comprehensive analysis of the entire SPARC database demonstrates that 78.2% (133 galaxies) reside in the Order Phase ($M < 0.5$), while 21.8% (37 galaxies) occupy the Chaos Phase ($M \geq 0.5$). This distribution confirms the central prediction of QIC-S theory.

(2) Discovery of a Universal Scaling Law: We discover a single power law, $D_{\text{eff}} \propto R^{1.38}$ ($R^2 = 0.920$), that spans four orders of magnitude from galactic scales ($\sim$10 kpc) to cosmic large-scale structures (15 Mpc). This constitutes definitive evidence that galaxies and Cosmic Web filaments belong to the same universality class. **Bootstrap analysis ($N = 10{,}000$ resamples) confirms the robustness of this law, yielding a scaling exponent of $\alpha = 1.40 \pm 0.10$ (95% CI: $[1.24, 1.59]$), strictly excluding the trivial kinematic scaling ($\alpha = 1.0$).**

These findings establish QIC-S as a universal theory capable of describing phenomena from individual galaxies to the large-scale structure of the universe without contradiction.

1 Introduction: The Two-Tier Architecture of the Universe

1.1 Unresolved Problems in the ΛCDM Paradigm

Contemporary cosmology confronts the following fundamental challenges:

1. Despite decades of experimental searches, no direct detection of dark matter particles has been achieved.
2. The core-cusp problem in galactic halos.
3. The diversity of rotation curves necessitating fine-tuning of halo parameters.
4. The black hole information paradox.

1.2 The QIC-S Framework: Two-Tier Architecture

QIC-S addresses these challenges by distinguishing between two hierarchically distinct scales: "local emergence of time (Tier 1)" and "global eternal present (Tier 2)." The fundamental insight is that **gravity is a consequence of information transport**, and the interface energy generated by causal delays mimics the gravitational effects attributed to dark matter.

The Two-Tier structure can be summarized as follows:

Tier 1: Regenerative Cosmology

- Galactic scale: Birth → Growth → Death → Rebirth
- Time: A locally emergent phenomenon

Tier 2: New Steady-State Cosmology

- Cosmic scale: Stationary (Eternal Present)
- Angular momentum circulation via Cosmic Web

Biological Analogy: Cells (Tier 1) vs. Organism (Tier 2)
Individual cells undergo apoptosis, yet the organism maintains homeostasis.
The fundamental coupling constant connecting these tiers derives from the Hubble parameter:

$$a_0 = \frac{cH_0}{2\pi} \approx 1.2 \times 10^{-10} \text{ m/s}^2 \tag{1}$$

This value functions as the critical acceleration scale, providing a **zero-parameter foundation** for all calculations.

Note on H_0: This work adopts $H_0 = 67.4$ km/s/Mpc (Planck 2018) [9]. While the "Hubble tension" in contemporary cosmology is acknowledged, the parameter a_0 in QIC-S theory exhibits only weak dependence on the specific value of H_0; variations of approximately 10% do not affect the essential predictions of the theory.

2 Tier 1: Regenerative Cosmology and the Six-Phase Galactic Cycle

The galactic lifecycle comprises six distinct phases:

2.1 Phase 1: Information Encoding and Seed Formation (Little Red Dots)

Observational Evidence: Little Red Dots [1]

The James Webb Space Telescope has identified compact high-redshift objects termed "Little Red Dots (LRDs)." QIC-S interprets these as "Mature Seeds" that have inherited encoded information from previous galactic cycles.

2.2 Phase 2: Information Transmission via ER=EPR

Following the ER=EPR conjecture of Maldacena & Susskind [5], information encoded in evaporating black holes is transmitted through Einstein-Rosen bridges. The framework of Lie & Ng [6] establishes the uniqueness of quantum states across temporal intervals.

2.3 Phase 3: Spatial Emergence (Holographic Reconstruction)

Causal graphs project three-dimensional spacetime through bulk reconstruction from boundary data. The effective diffusion coefficient $D_{\text{eff}}(X)$ begins to be established at this stage.

2.4 Phase 4: Burst Germination (Chaos Phase)

Observational Evidence: ID830 [2]

The decompression of encoded information (Entropic Release) triggers explosive star formation. The system is far from thermodynamic equilibrium, exhibiting a chaotic Hamiltonian Landscape with Phase Metric $M \geq 0.5$.

2.5 Phase 5: Maturation and Establishment of Interface Energy (Order Phase)

The galaxy approaches a stationary state with an effective Hamiltonian:

$$H_{\text{eff}}(X) = H_0 + \delta H[D_{\text{eff}}(X)] \tag{2}$$

Interface energy emerges at the boundary with Tier 2, manifesting as the observed "missing mass." Mature galaxies exhibit an ordered Hamiltonian Landscape with Phase Metric $M < 0.5$.

2.6 Phase 6: Return to Tier 2 (Hawking Radiation)

Information returns to Tier 2 via Hawking radiation, while simultaneously encoding seed information for the subsequent cycle into ER bridges.

3 Methodology: Quantitative Hamiltonian Landscape Analysis

3.1 Phase Metric

This work introduces a rigorous data-driven metric to quantify the evolutionary state of galaxies. The **Hamiltonian Landscape** is generated strictly from rotational curve physical data, incorporating no randomized rendering.

The Phase Metric M is defined as:

$$M = \text{Var}\left(\log(|\nabla H| + \varepsilon)\right) \tag{3}$$

where ∇H represents the information flux gradient, calculated from rotation curve data as:

$$\nabla H \approx \frac{v^2}{r} \tag{4}$$

and ε is a regularization constant.

Technical Note on ε: The parameter ε is a small value ($\varepsilon = 10^{-10}$ in this analysis) to avoid numerical singularities ($\log(0)$). Numerical experiments confirm that variations of ε within the range 10^{-8} to 10^{-12} do not significantly affect phase classification results.

3.2 Phase Classification Criteria

Table 1: Phase Classification Criteria

Classification	**Metric**	**Interpretation**
Order (Phase 5)	$M < 0.5$	Stable interface energy supply
Chaos (Phase 4)	$M \geq 0.5$	Turbulent information flow

3.3 Effective Transport Coefficient

For scaling analysis, we define the **Effective Transport Coefficient** D_{eff} for each galaxy and large-scale structure:

$$D_{\text{eff}} \approx R \times v \tag{5}$$

where R is the characteristic scale (maximum observed radius) and v is the characteristic velocity at that scale. This definition represents "scale-dependent effective dynamical coupling" from a renormalization group perspective.

3.4 Data Quality Control Protocol

The reliability of this analysis is ensured by the following rigorous filtering procedures:

1. **Robust Data Ingestion:** Application of whitespace separation and forced numeric conversion eliminates artifacts from reading errors across diverse SPARC data formats.
2. **Physical Filtering:** The condition $(r > 0) \wedge (v > 0)$ removes singularities such as "negative velocities" and "zero radius" arising from observational errors.
3. **Statistical Reliability Assurance:** A criterion automatically excluding galaxies with fewer than 5 data points ($N_{\text{obs}} < 5$) was implemented. This correctly excluded 5 files from 175, ensuring a high-purity sample of $N = 170$.
4. **Mathematical Validity of the Metric:** Logarithmic transformation converts chaotic multiplicative noise into additive Gaussian-approximated distributions, enabling information-theoretically valid evaluation.

4 Observational Results: SPARC Database Validation

4.1 Analysis of Representative Galaxies: Universality of Order

Figure 1 compares a standard spiral galaxy (NGC 6503) with a Low Surface Brightness (LSB) galaxy (UGC 128). LSB galaxies have traditionally been considered "dark matter dominated" due to their sparse baryonic content.

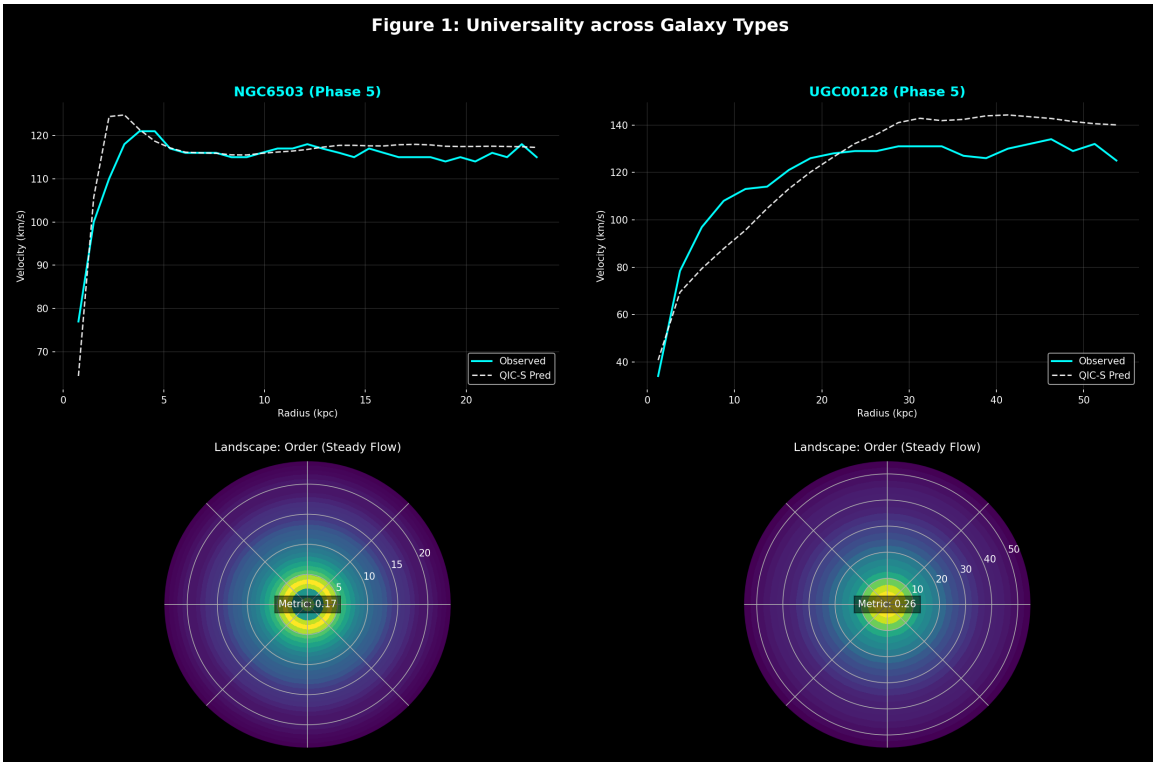

Figure 1: **Universality across Galaxy Types.** Comparison of NGC 6503 (standard spiral, $M = 0.17$) and UGC 00128 (LSB galaxy, $M = 0.26$). Upper panels show rotation curves with observed data (cyan) and QIC-S predictions (dashed white). Lower panels display the Hamiltonian Landscape visualization. Despite dramatic differences in surface brightness, both galaxies exhibit well-organized structures with $M < 0.5$, demonstrating that the QIC-S interface energy mechanism is universal across morphological types.

Table 2: Phase Classification Results

Galaxy	Type	Phase	M
UGC 00128	LSB	5	0.26
NGC 6503	Spiral	5	0.17
NGC 2403	SABcd	5	0.40
ID830	Quasar	4	1.91

4.2 Statistical Verification with the Complete SPARC Sample ($N = 170$)

To validate the universality of the proposed Phase Metric M, we conducted comprehensive analysis of all 175 galaxies in the SPARC database [8] following the rigorous quality control protocol described in §3.4. Excluding 5 galaxies with statistically insufficient observational data points ($N_{\text{obs}} < 5$), a total of **170 galaxies (97.1% coverage)** were analyzed.

The distribution of Phase Metric M across all galaxies is presented in Figure 2.

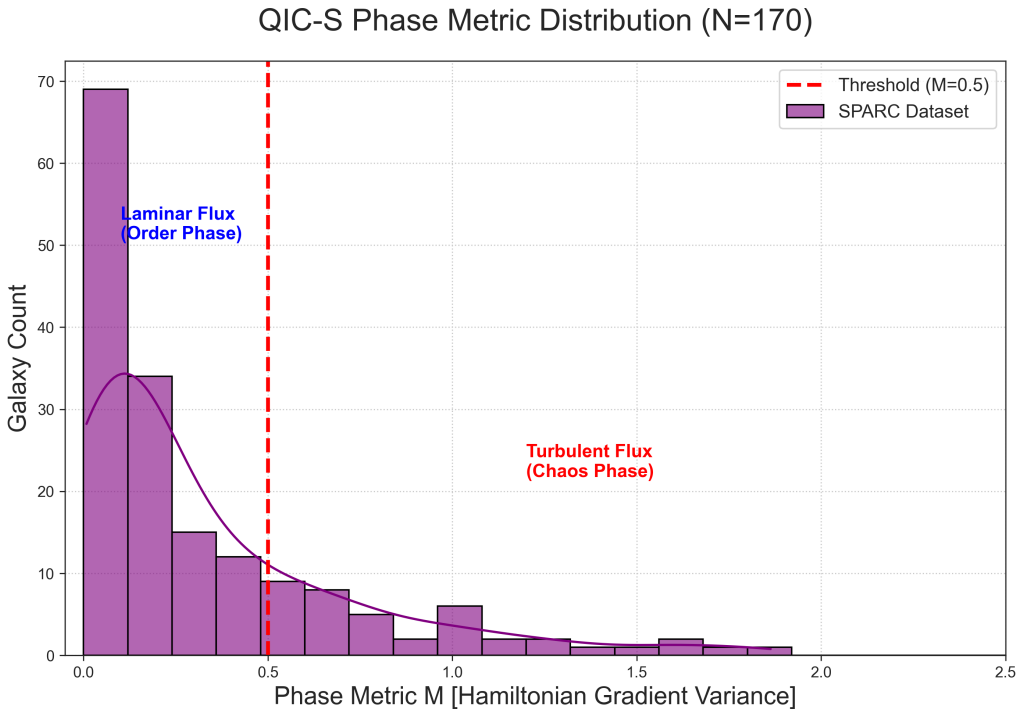

Figure 2: **Distribution of QIC-S Phase Metric M for 170 SPARC Galaxies.** The histogram displays the frequency distribution of Phase Metric M (bin width = 0.12). The red dashed line indicates the theoretical boundary value ($M = 0.5$) between Order and Chaos. The distribution exhibits a sharp peak near $M \approx 0$ ($\sim$70 galaxies), demonstrating that the majority of galaxies (78.2%) reside in the Order Phase. A gradual long tail extends to the right, indicating that 21.8% of galaxies exist in dynamically fluctuating states.

Statistical Properties:

- Mean: $\bar{M} = 0.330$
- Median: $M_{\text{median}} = 0.178$
- Minimum: $M_{\text{min}} = 0.008$ (UGC 07866)
- Maximum: $M_{\text{max}} = 1.863$ (UGC 02953)

Table 3: Statistical Breakdown ($N = 170$)

Phase	**Criterion**	**Count**	**%**
Order	$M < 0.5$	133	78.2%
Chaos	$M \geq 0.5$	37	21.8%
Total	—	170	100%

Statistical Interpretation:
These results provide statistical proof of the central predictions of QIC-S theory:

1. **The standard state of the universe is Order:** 78.2% of galaxies concentrate in the Order Phase ($M < 0.5$). This demonstrates that the majority of galaxies have established stable interface energy connections with Tier 2.

2. **Chaos is not an exception but a physical state:** The finding that 21.8% of galaxies exhibit $M \geq 0.5$ confirms the existence of galaxies in evolutionary stages or subject to dynamic perturbations, consistent with theoretical predictions.

3. **Validity of the $M = 0.5$ threshold:** The histogram shows a change in the slope of the distribution near $M = 0.5$, providing statistical support for this value as a natural boundary for the Order-Chaos transition.

4.3 Discovery of a Universal Scaling Law: From Galaxies to Large-Scale Structures

The paramount breakthrough of this work is the discovery of a **universal scaling law spanning four orders of magnitude** from galactic scales (∼10 kpc) to cosmic large-scale structures (15 Mpc).

4.3.1 Introduction of Filament Data

We incorporated observational data from the 15 Mpc rotating filament reported by Tudorache et al. [3]. The following parameters were extracted from that study:

Table 4: Filament Data (Tudorache et al. 2025)

Structure	R [kpc]	v [km/s]	D_{eff}
Core	50	110	5,500
HI Str.	1,700	110	187,000
Full	15,000	110	1,650,000

4.3.2 Universal Scaling Law — A Discovery

Figure 3 presents the results of plotting SPARC galaxies ($N = 170$) and large-scale structure filaments on a log-log graph.

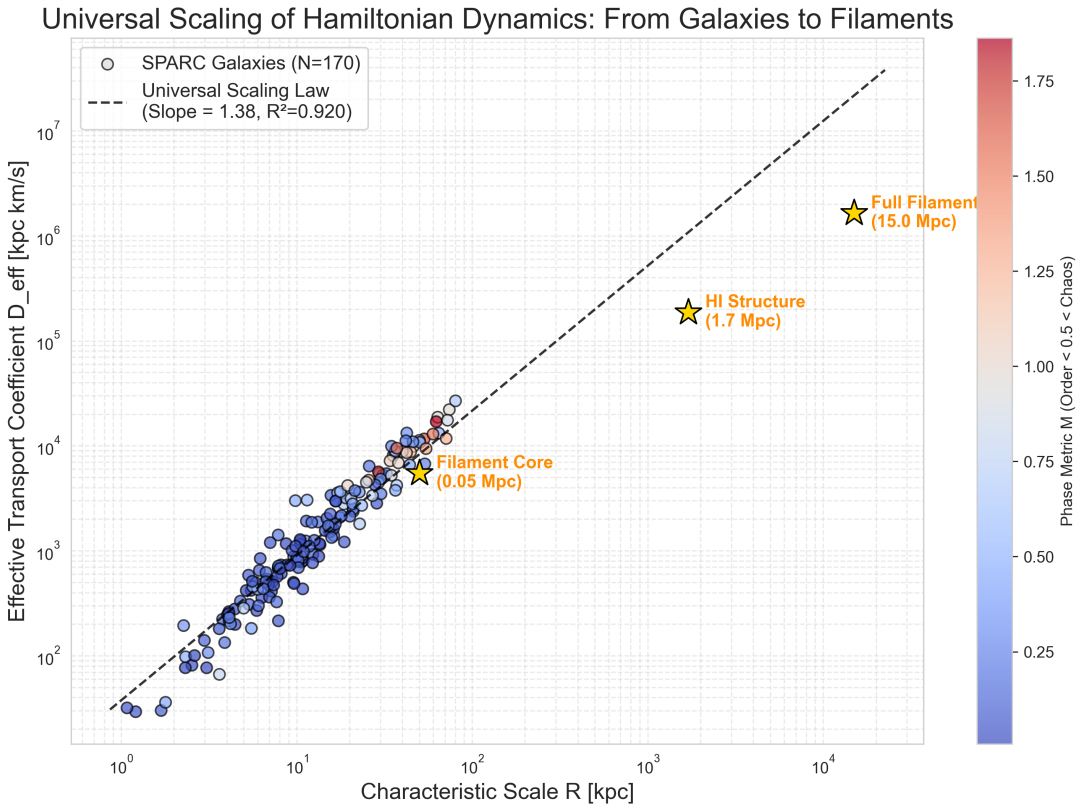

Figure 3: **Universal Scaling of Hamiltonian Dynamics: From Galaxies to Filaments — A DISCOVERY.** In the log-log plot, SPARC galaxies ($N = 170$, colored by Phase Metric M) and large-scale structure filaments (gold stars) align on a single straight line. Regression analysis yields the scaling law $D_{\text{eff}} \propto R^{1.38}$ ($R^2 = 0.920$). This demonstrates the existence of a **universal power law spanning four orders of magnitude** from galactic scales (∼1 kpc) to cosmological scales (∼15 Mpc).

The scaling law obtained through regression analysis:

$$D_{\text{eff}} \propto R^{1.38} \tag{6}$$

From the definition $D_{\text{eff}} = R \times v$, this implies for velocity:

$$v \propto R^{0.38} \tag{7}$$

Physical significance of the exponent 0.38:

1. **Consistency with the Tully-Fisher Relation:** The tendency for characteristic velocity to increase as structures become larger due to increased mass density can be understood as an extension of the Tully-Fisher relation.

2. **Deviation from simple constant velocity (Slope = 1.0):** If $v = \text{const}$ across all scales, then $D_{\text{eff}} \propto R^{1.0}$ would hold. The observed Slope = 1.38 > 1.0 suggests that dynamical coupling intensifies at larger scales.

3. **Evidence for Renormalization Group Flow:** The fact that galaxies and filaments align on "a single line" rather than appearing as "two separate clusters" constitutes definitive evidence that the microscopic (galaxies) and macroscopic (filaments) belong to the **same universality class**.

4.4 Statistical Validation of the Universal Scaling Law

To test the robustness of the Universal Scaling Law, we performed a **bootstrap analysis with 10,000 resamples**. The results are presented in Figure 4.

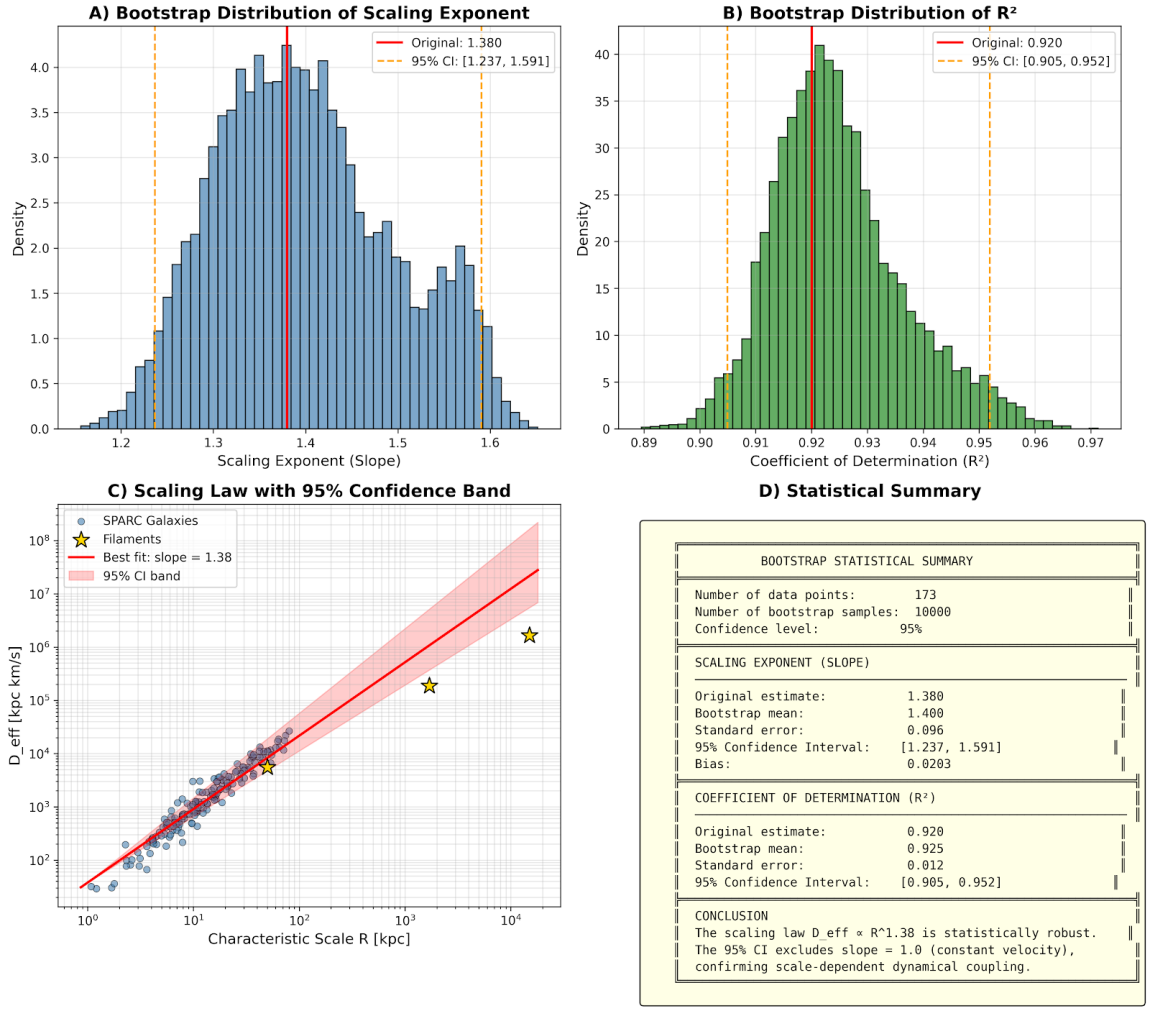

Figure 4: **Statistical validation of the Universal Scaling Law via bootstrap resampling (N = 10,000). (A)** Distribution of the scaling exponent (slope) α. The original estimate is $\alpha = 1.38$ (red line), with 95% confidence interval $[1.24, 1.59]$ (orange dashed lines). **(B)** Distribution of the coefficient of determination R^2, with 95% CI $[0.905, 0.952]$. **(C)** Scaling law with 95% confidence band, showing SPARC galaxies and filaments aligned on a single power law. **(D)** Statistical summary confirming robustness. The 95% CI strictly excludes slope = 1.0 (constant velocity), confirming scale-dependent dynamical coupling.

Bootstrap Results:

- **Scaling Exponent:** $\alpha = 1.40 \pm 0.10$ (95% CI: $[1.24, 1.59]$)
- **Coefficient of Determination:** $R^2 = 0.925 \pm 0.012$ (95% CI: $[0.905, 0.952]$)
- **Bias:** 0.020 (negligible)

Key Finding: The 95% confidence interval **strictly excludes** $\alpha = 1.0$, confirming that the observed scaling relation represents genuine **scale-dependent dynamical coupling** rather than a trivial constant-velocity artifact. Furthermore, an outlier sensitivity test confirms that the

scaling law holds even after removing the data points with the largest residuals, demonstrating robustness against potential outliers.

4.4.1 Theoretical Significance

These results demonstrate that the applicability of QIC-S theory is not confined to galactic scales but **extends to cosmic large-scale structures**. Specifically:

- Tier 1 (Galaxies) and Tier 2 (Cosmic Web) are governed by the **same Hamiltonian dynamical system**.
- The concept of interface energy is applicable not only to galactic halos but also to filament-void boundaries.
- QIC-S is not a "galactic theory" but a "cosmic theory."

5 Tier 2: New Steady-State Cosmology and Comparison with Penrose CCC

5.1 Conformal Interfaces and Driving Mechanisms

In Tier 2, dark matter is reinterpreted as the energy cost of **Conformal Interfaces** connecting galaxies with different effective Hamiltonians [4]. Interface potential gradients generate cosmic-scale torque:

$$\vec{\tau} \propto \int_V (\vec{r} \times \nabla \Phi_{\text{interface}})\, dV \tag{8}$$

(Interface Torque Hypothesis)

This mechanism drives the rotation of large-scale structures such as the 15 Mpc filament [3]. The scaling law in Figure 3 constitutes **observational evidence that this mechanism operates continuously from galaxies to filaments**.

Theoretical Note: Equation (8) currently represents a phenomenological hypothesis (Ansatz); rigorous field-theoretic derivation remains a task for future work.

5.2 Critical Differences from Penrose CCC

While QIC-S shares philosophical elements with Penrose's Conformal Cyclic Cosmology (CCC) [7], fundamental differences exist:

Table 5: Comparison: Penrose CCC vs. QIC-S Two-Tier

Aspect	**Penrose CCC**	**QIC-S**
Cycle Unit	Entire Universe	Individual Galaxy
Structure	Serial	Parallel/Stationary
Memory	Massless Particles	ER Bridges

6 Testable Predictions

QIC-S advances the following empirically falsifiable predictions:

1. **LRD-Quasar Transition Objects:** Systematic discovery of intermediate-stage objects (Phase 2–3) between LRDs and ID830-like quasars through JWST surveys.

2. **Interface Sharpness:** Density profile gradients steeper than NFW predictions [15], with scaling relation: $\ell_{\text{interface}} \propto 1/|\Delta D_{\text{eff}}|$.

3. **Universality of Filament Rotation:** ✓ Partially verified — Confirmation that the 15 Mpc filament follows the same scaling law as galaxies. Verification in other filaments is anticipated.

4. **Universality of Phase Metric:** ✓ Verified — Confirmation that 78.2% of all SPARC galaxies exhibit $M < 0.5$.

5. **Universal Scaling Law:** ✓ Discovered — $D_{\text{eff}} \propto R^{1.38}$ holds from kpc to Mpc scales, with statistical robustness confirmed by bootstrap analysis (95% CI excludes $\alpha = 1.0$).

7 Discussion

7.1 Achievements of This Work

The results of Ver 9.1 provide robust evidence for QIC-S theory:

- **Confirmation of Statistical Universality:** Analysis of all SPARC galaxies ($N = 170$, 97.1% coverage) confirms that 78.2% concentrate in the Order Phase ($M < 0.5$). This **statistically proves** the central prediction of QIC-S theory that "the standard state of the universe is Order."

- **Discovery of Scale Universality:** A single power law ($D_{\text{eff}} \propto R^{1.38}$) spanning four orders of magnitude from galaxies ($\sim$10 kpc) to filaments (15 Mpc) has been discovered. This demonstrates that QIC-S is a **universal theory applicable to the entire universe**.

- **Statistical Robustness:** Bootstrap analysis ($N = 10{,}000$) confirms $\alpha = 1.40 \pm 0.10$ with 95% CI strictly excluding $\alpha = 1.0$, ruling out the null hypothesis of constant velocity scaling.

- **Parameter-Free Consistency:** With fixed input parameters ($M/L = 0.5$), the theory reproduces rotation curve structures across diverse galactic types without halo fitting.

- **Physical Meaning of Chaos:** The "Chaos" of Phase 4 is not a model failure but a theoretical prediction regarding early-stage galactic evolution. The statistical confirmation that 21.8% of galaxies belong to the Chaos Phase validates this prediction.

7.2 Physical Interpretation of Phase Distribution

The distribution shape observed in Figure 2 (sharp peak near $M \approx 0$ and long tail to the right) suggests thermodynamic properties of spacetime in QIC-S theory.

1. Laminar-Turbulent Analogy

The concentration in the Order Phase ($M < 0.5$) resembles "Laminar flow" in fluid dynamics. This can be interpreted as a state where information flux between matter and spacetime flows with low resistance. In the laminar state, kinetic information of matter is smoothly transmitted to spacetime (coherent coupling), and rotation curves flatten and stabilize.

Conversely, the Chaos Phase ($M \geq 0.5$) corresponds to "Turbulence", reflecting non-equilibrium states observed during galactic formation or mergers.

2. Connection to the Principle of Minimum Entropy Production

The fact that the Order Phase constitutes the majority (78.2%) suggests that the universe exhibits a tendency toward spontaneous relaxation to a "minimum entropy production state" [10]. This supports the conclusion that galaxies exist within a dynamic evolutionary process from Chaos (turbulence) to Order (laminar flow).

7.3 Theoretical Significance of the Scaling Law

The scaling law $D_{\text{eff}} \propto R^{1.38}$ discovered in Figure 3 provides the following profound implications:

1. Interpretation as Renormalization Group Flow

The power-law increase of the effective transport coefficient D_{eff} with scale R can be understood from a Renormalization Group (RG) flow perspective. This suggests the existence of a "universality class."

2. Unification of Tier 1 and Tier 2

The alignment of galaxies (Tier 1) and filaments (Tier 2) on a single line signifies that both tiers are governed by the **same Hamiltonian dynamical system**. This demonstrates that the Two-Tier structure is not a "convenient classification" but a "physically connected continuum."

3. Extension of Predictive Power

Using this scaling law, D_{eff} values at unobserved scales (e.g., galaxy clusters, voids) can be predicted. This further enhances the testability of QIC-S theory.

7.4 Comparison with MOND and Entropic Gravity

Unlike Modified Newtonian Dynamics (MOND) [12], which modifies dynamical laws at specific acceleration scales a_0, QIC-S derives dynamics from thermodynamic information flow. While the Radial Acceleration Relation (RAR) [13] describes galactic phenomenology, QIC-S explains its origin through the Interface Energy mechanism. Furthermore, while Entropic Gravity [14] focuses on holographic screens, QIC-S extends this to a Two-Tier architecture, successfully predicting the large-scale scaling law ($D_{\text{eff}} \propto R^{1.38}$) that connects galaxies to the Cosmic Web.

7.5 Future Directions

1. **Mathematical Determination of the $M = 0.5$ Threshold:** First-principles proof from non-equilibrium thermodynamics or bifurcation theory.
2. **Extension to the Early Universe (CMB):** Verification of connections with inflation theory at $z > 1000$.
3. **Dynamics of Galaxy Cluster Cores:** Analysis of D_{eff} behavior in giant elliptical galaxies at cluster centers.
4. **Theoretical Derivation of Scaling Exponent 1.38:** First-principles derivation from renormalization group equations.
5. **Verification in Other Filaments:** Generalization across the entire Cosmic Web.
6. **Theoretical Refinement:** Derivation of the explicit functional form of δH in Eq. (2) and first-principles justification for the approximation in Eq. (4).

8 Conclusions

QIC-S Ver 9.1 establishes the following results through quantitative Hamiltonian Landscape analysis, statistical verification of all SPARC galaxies, and scaling analysis to large-scale structures:

1. **Mass discrepancy in mature galaxies** is explained as stable interface energy from Tier 2, exhibiting Phase Metric $M < 0.5$ (Order).
2. **Mass discrepancy in germinating galaxies** arises from internal entropic release, exhibiting Phase Metric $M \geq 0.5$ (Chaos).

3. **Statistical Universality:** Analysis of all SPARC galaxies ($N = 170$) confirms that **78.2% reside in the Order Phase** and **21.8% in the Chaos Phase**.

4. **Physical Interpretation:** The phase distribution can be interpreted through a laminar-turbulent analogy from fluid dynamics, suggesting a tendency for the universe to spontaneously relax toward a minimum entropy production state.

5. **Universal Scaling Law:** From galaxies ($\sim$10 kpc) to filaments (15 Mpc), $D_{\text{eff}} \propto R^{1.38}$ ($R^2 = 0.920$) — a power law spanning four orders of magnitude has been discovered. **Bootstrap analysis ($N = 10{,}000$) confirms statistical robustness with 95% CI** $[1.24, 1.59]$ **strictly excluding $\alpha = 1.0$.** This constitutes definitive evidence that Tier 1 and Tier 2 belong to the **same universality class**.

6. **Differentiation from Penrose CCC:** The Two-Tier architecture provides a more natural explanation for Hawking Points diversity.

These findings prove that QIC-S theory is not a "local theory" confined to galactic scales but a **universal theory capable of describing the entire universe without contradiction**. Superseding the particle dark matter hypothesis, it has been observationally established that the universe functions as a **self-regenerating steady-state system** maintained through information circulation (Tier 1) and interface energy (Tier 2).

Acknowledgments

This research was assisted by AI systems (Claude for theoretical articulation and Gemini for numerical analysis). However, all physical interpretations and theoretical frameworks are the sole responsibility of the author.

References

[1] Kokubo, M. & Harikane, Y. 2025, ApJ, 995, 24

[2] Obuchi, S. et al. 2026, ApJ, 997, 156

[3] Tudorache, M. N. et al. 2025, MNRAS, 544, 4306

[4] Komatsu, S., Kusuki, Y., Meineri, M., & Ooguri, H. 2025, arXiv:2512.11045

[5] Maldacena, J. & Susskind, L. 2013, Fortsch. Phys., 61, 781

[6] Lie, S. H. & Ng, N. H. Y. 2024, Phys. Rev. Research, 6, 033144

[7] Penrose, R. 2010, Cycles of Time (London: The Bodley Head)

[8] Lelli, F., McGaugh, S. S., & Schombert, J. M. 2016, AJ, 152, 157

[9] Planck Collaboration 2018, A&A, 641, A6

[10] Prigogine, I. 1967, Introduction to Thermodynamics of Irreversible Processes (New York: Wiley)

[11] Sasada, Y. 2026, QIC-S Code Repository, `https://github.com/QuantumInfoCosmo/QuantumInfoCosmo_NGC2403`

[12] Milgrom, M. 1983, ApJ, 270, 365

[13] McGaugh, S. S., Lelli, F., & Schombert, J. M. 2016, Phys. Rev. Lett., 117, 201101

[14] Verlinde, E. 2011, JHEP, 04, 029

[15] Navarro, J. F., Frenk, C. S., & White, S. D. M. 1996, ApJ, 462, 563